JOURNAL OF VIROLOGY, July 2005, p. 8742–8749 Vol. 79, No. 14
0022-538X/05/$08.00+0 doi:10.1128/JVI.79.14.8742–8749.2005

Activation of the N-Ras–PI3K–Akt–mTOR Pathway by Hepatitis C Virus: Control of Cell Survival and Viral Replication

Petra Mannová and Laura Beretta*

Public Health Sciences Division, Fred Hutchinson Cancer Research Center, Seattle, Washington 98109

Received 16 November 2004/Accepted 16 March 2005

The hepatitis C virus (HCV) replication complex is localized within detergent-resistant membranes or lipid rafts. We analyzed the protein contents of detergent-resistant fractions isolated from Huh7 cells expressing a self-replicating full-length HCV-1b genome. Using two-dimensional gel electrophoresis followed by mass spectrometry, we identified N-Ras as one of the proteins in which expression was increased in the detergent-resistant fractions from HCV genomic replicon clones compared to control cells. N-Ras is an activator of the phosphatidylinositol-3-kinase (PI3K)-Akt pathway. We found that the activities of PI3K and Akt, as well as the activity of their downstream target, mTOR, in the HCV-replicating cells were increased. Both PI3K-Akt- and mTOR-dependent pathways have been shown to promote cell survival. In agreement with this, HCV replicon cells were resistant to serum starvation-induced apoptosis. We also characterized the role of this pathway in HCV replication. Reduction of N-Ras expression by transfection of N-Ras small interfering RNA (siRNA) resulted in increased replication of HCV. We observed a similar increase in HCV replication in cells treated with the PI3K inhibitor LY294002 and in cells transfected with mTOR siRNA. Taken together, these data suggest that increased N-Ras levels in subcellular sites of HCV replication and stimulation of the prosurvival PI3K-Akt pathway and mTOR by HCV not only protect cells against apoptosis but also contribute to the maintenance of steady-state levels of HCV replication. These effects may contribute to the establishment of persistent infection by HCV.

Hepatitis C virus (HCV) is a small, enveloped plus-strand RNA virus in the genus *Hepacivirus* and the family *Flaviviridae*. In the majority of infected individuals, HCV establishes a persistent infection with high subsequent risks of liver cirrhosis and hepatocellular carcinoma. A major drawback in studying the HCV life cycle is the lack of an in vitro system allowing production of infectious particles. However, the generation of subgenomic and genomic HCV replicons harboring cell culture-adaptive mutations enabled replication of HCV RNA in the Huh7 hepatoma cell line (5, 24, 28).

Replication of HCV is accompanied by the formation of intracellular membranes called a membranous web (18). The precise character of these membranes remains to be determined, but there is a growing body of evidence that active replication complexes of HCV reside in lipid raft domains of these membranes. The nonstructural HCV proteins and the plus and minus RNA strands of HCV were found to be associated with caveolin-2, a lipid raft marker, in the detergent-resistant subcellular fraction (35). HCV replication complexes may be protected within lipid rafts, as HCV RNA and nonstructural proteins are resistant to RNase and protease digestion (1). In addition, depletion of cellular cholesterol selectively reduced HCV RNA replication (1). Raft domains are involved in intracellular trafficking and construction of signaling complexes (22, 36). Therefore, lipid rafts represent a potential compartment, the targeting of which may allow viruses to perturb cell signaling pathways (3, 25). These specialized subcellular membrane domains have also been shown to play important roles in the replication cycles of other viruses, from cell entry to assembly and budding (6–8, 11, 34, 38, 39).

In this study, we used a proteomic approach to characterize the protein content of the HCV replication complex-containing lipid raft fraction in order to identify signaling pathways targeted by HCV.

MATERIALS AND METHODS

Cell culture. Human hepatoma Huh7 cells were grown in Dulbecco's modification of Eagle's medium (DMEM) supplemented with 10% fetal bovine serum (FBS) (cellgro/Mediatech) and 1% penicillin-streptomycin (Invitrogen). The Huh7 clone T1, stably expressing the neomycin resistance gene, was described previously (17). Stable Huh7 clones expressing the selectable full-length (sfl) HCV-1b genome were generated by transfection of the sfl construct (28), kindly provided by Ralf Bartenschlager. In vitro transcription of sfl plasmid was performed as described previously (24). Huh7 cells (8×10^6) were electroporated with 2 μg of in vitro transcripts in OPTI-MEM (Invitrogen) and 1.25% dimethyl sulfoxide. Twenty-four hours posttransfection, 800 μg/ml of G418 (Invitrogen) was added to the culture medium. Three weeks later, growing colonies were isolated and subcloned in complete DMEM with 400 μg/ml of G418. The generated stable cell clones, SFL-2 and SFL-3, as well as the control T1 clone, were grown in complete DMEM with G418 (400 μg/ml). For transient transfection, Huh7 cells cultured in six-well plates were incubated with 1 ml OPTI-MEM (Invitrogen), 8 μl DMRIE-C (Invitrogen), and 5 μg of in vitro-transcribed sfl construct for 4 h. Transfected cells were cultured in DMEM for 48 h before lysis.

Flotation assay. To isolate detergent-insoluble membrane domains, approximately 2×10^8 of Huh7, T1, SFL-2, and SFL-3 cells were washed with cold phosphate-buffered saline (PBS), lysed in 1.5 ml of hypotonic buffer (10 mM Tris-HCl, pH 7.5, 10 mM KCl, 5 mM $MgCl_2$), and broken by being passed through a 25-gauge needle 20 times. Nuclei were removed by centrifugation at $1{,}000 \times g$ for 5 min at 4°C. Postnuclear supernatants were treated with 1% NP-40 for 20 min on ice and mixed with 15 ml of 72% sucrose in low-salt buffer (LSB) (50 mM Tris-HCl, pH 7.5, 25 mM KCl, 5 mM $MgCl_2$). Each 5.5 ml of the mix was overlaid with 5 ml of 55% sucrose–LSB and 1.5 ml of 10% sucrose–LSB. Sucrose gradients were centrifuged at 35,000 rpm in a Beckman SW41 Ti rotor for 18 h at 4°C. Fractions were collected from the top of the gradient (1 ml for fraction 1 and 1.5 ml for subsequent fractions). Fractions were concentrated by centrifugation through 10 kDa PES Vivaspin columns (Vivascience).

* Corresponding author. Mailing address: Fred Hutchinson Cancer Research Center, 1100 Fairview Ave. North, M5-A864, Box 19024, Seattle, WA 98109-1024. Phone: (206) 667-7080. Fax: (206) 667-2537. E-mail: lberetta@fhcrc.org.

Two-dimensional (2-D) gel electrophoresis and mass spectrometry analysis. To remove lipids, samples were precipitated with acetone–10% trichloroacetic acid–0.07% beta-mercaptoethanol for 2 h at −20°C. Precipitates were briefly centrifuged, washed with acetone–0.07% beta-mercaptoethanol, air dried, and solubilized in 6 M urea, 2 M thiourea, 2% NP-40, and 2% beta-mercaptoethanol supplemented with 1% ASB-14. Each protein sample (120 μg) was supplemented with 2% ampholytes (pH 4 to 8; Gallard/Schlessinger) and applied on the isofocusing first-dimension gel. Isoelectric focusing was carried out at 700 V for 16 h followed by 1,000 V for 2 h. Gels were equilibrated in 125 mM Tris, pH 6.8, 10% glycerol, 2% sodium dodecyl sulfate (SDS), 1% dithiothreitol, and bromophenol blue and loaded onto the gradient (11 to 14%) polyacrylamide second-dimension gel. After separation, proteins were visualized by a photochemical silver-based staining. The gels were digitized with a Kodak CCD camera, and spots were quantified using BioImage 2-D Analyzer software. The spot of interest was excised and destained in 15 mM potassium ferricyanide and 50 mM sodium thiosulfate for 10 min, followed by three washes with water and dehydration in 100% acetonitrile for 5 min. The proteins were digested in gel with trypsin (Promega) in 200 mM sodium bicarbonate at 37°C overnight. Peptides were extracted twice with 10% acetonitrile–10% formic acid, centrifuged, and resuspended in 5% acetonitrile–0.1% formic acid. Peptides were analyzed by nanoflow capillary liquid chromatography coupled with electrospray quadrupole time-of-flight tandem mass spectrometry (LC-ESI/Q-TOF MS-MS) in the Q-TOF micro (Waters, Manchester, United Kingdom). ESI/Q-TOF MS-MS tandem spectra were recorded in the automated MS to MS-MS switching mode with an *m/z*-dependent set of collision offset values. The acquired spectra were processed and searched against a nonredundant SwissProt protein sequence database.

SDS-PAGE and Western blotting. Cells were lysed in 50 mM Tris-HCl, pH 8, 150 mM NaCl, 0.1% SDS, 1% NP-40, and 1.6 μg/ml of aprotinin or directly in Laemmli sample buffer. When indicated, cells were treated with 10 or 50 μM phosphatidylinositol-3-kinase (PI3K) inhibitor LY294002 (Cell Signaling Technology) before lysis. Proteins were resolved on 5%, 10%, 12%, or 15% SDS-polyacrylamide gel electrophoresis (PAGE) and electrotransferred onto a nitrocellulose membrane (Amersham Biosciences). Membranes were blocked with 5% nonfat milk in 10 mM Tris-HCl, pH 7.5, 2.5 mM EDTA, pH 8, 50 mM NaCl, and incubated with primary antibodies overnight. The following antibodies were used: anti-NS5A monoclonal antibody (ViroStat), monoclonal anti-NS5B antibody 3B1 (kindly provided by Darius Moradpour), anti-caveolin-2 goat polyclonal antibody (Santa Cruz Biotechnology), anti-N-Ras monoclonal antibody (Santa Cruz Biotechnology), monoclonal anti-actin antibody (MP Biomedicals), anti-BiP polyclonal antibody (Santa Cruz Biotechnology), anti-Akt polyclonal antibody (Cell Signaling Technology), anti-phospho-Akt (Ser473) polyclonal antibody (Cell Signaling Technology), anti-mTOR polyclonal antibody (Cell Signaling Technology), anti-4E-BP1 polyclonal antibody (Cell Signaling Technology), anti-phospho-4E-BP1 (Thr70) polyclonal antibody (Cell Signaling Technology), anti-phospho-p70 S6 kinase (Thr389) monoclonal antibody (Cell Signaling Technology), anti-p70 S6 kinase polyclonal antibody (Cell Signaling Technology), and anti-caspase-3 polyclonal antibody (Cell Signaling Technology). Horseradish peroxidase-conjugated immunoglobulins (DAKO) were used as secondary antibodies and proteins were visualized with ECL chemiluminescent reagent (Amersham Biosciences). Quantification of immunodetected protein bands was performed using ImageJ software (Research Services Branch/National Institute of Mental Health/National Institutes of Health).

siRNA. SFL-2 and SFL-3 cells were transfected with 50 nM siRNA specific to N-Ras (Santa Cruz Biotechnology), 100 nM siRNA specific to mTOR (Cell Signaling Technology), 100 nM nontargeting siRNA (Dharmacon) or were mock transfected according to the manufacturer's protocol (Santa Cruz Biotechnology). Thirty hours posttransfection, cells were lysed and proteins were analyzed by Western blotting. In parallel experiments, total RNA was purified with Trizol (Invitrogen) as recommended by the manufacturer's protocol and used for real-time PCR analysis.

Real-time PCR. One microgram of DNAse1-treated total RNA was reverse transcribed by using Moloney murine leukemia virus reverse transcriptase (Invitrogen) and antisense primer for 50 min at 42°C following heat inactivation of reverse transcriptase. cDNA mixtures (1/100) were treated with RNase H at 37°C for 30 min and mixed with an equal volume of 2 × iQ SYBR green supermix (Bio-Rad Laboratories) and the following primers specific for the conservative 5′ noncoding region in the HCV genome: 5′-CTCGCAAGCCACCCTATCAGG CAGTA-3′ (antisense) and 5′-CGGGAGAGCCATAGTGGTCTGCG-3′ (sense). Reactions were performed with the iCycler MyiQ real-time PCR detection system and analyzed by MyiQ software (Bio-Rad Laboratories). Actin quantifications (by use of random-primed cDNAs and primers 5′-TGGACTTCGAGCAAG AGATGG-3′ and 5′-GGAAGGAAGGCTGGAAGAGTG-3′) were performed for internal controls.

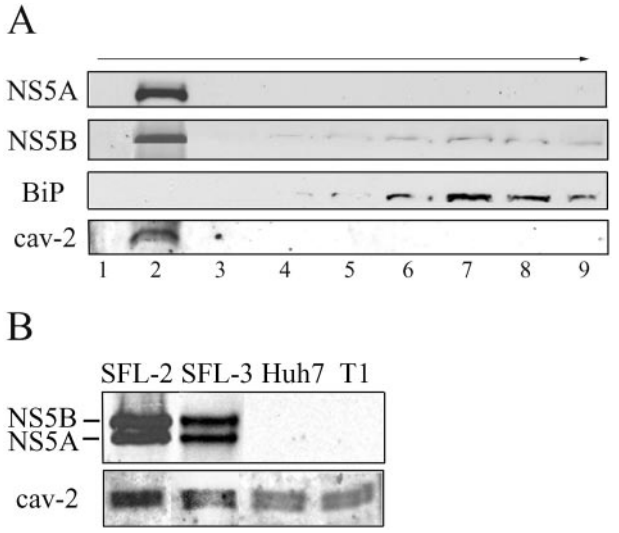

FIG. 1. Isolation and separation of detergent-resistant membrane fractions by flotation assay. (A) HCV proteins NS5A and NS5B were detected predominantly in fraction 2, which contained caveolin-2 (cav-2), a cellular marker of detergent-insoluble membrane domains. The endoplasmic reticulum protein BiP was detected in heavier fractions. (B) Expression of the HCV protein NS5A and NS5B in detergent-resistant membrane fractions isolated from full-length HCV replicon cell lines (SFL-2 and SFL-3) and control cell lines Huh7 and T1. NS5A, NS5B, and caveolin-2 (cav-2) were detected by Western blotting.

Apoptosis assays. Cells plated on glass coverslips were incubated in DMEM without FBS for 72 h. For Hoechst dye staining, cells were fixed with 4% paraformaldehyde in PBS at 4°C for 1 h, washed with PBS, and stained with Hoechst 33258 dye (8 μg/ml) at 37°C for 30 min. Cells with bright, condensed nuclei were scored as apoptotic by using a fluorescence microscope (Nikon E800). A total of 1,000 cells for each cell line were counted in randomly selected fields. For the terminal deoxynucleotidyltransferase-mediated dUTP nick end labeling (TUNEL) assay, cells were fixed with 4% paraformaldehyde in PBS at room temperature for 1 h, permeabilized with 0.1% Triton X-100 in 0.1% sodium citrate at 4°C for 2 min, and rinsed with PBS. TUNEL was performed with In Situ Cell Death Detection Kit, Fluorescein (Roche Applied Science), according to the manufacturer's protocol. TUNEL-positive cells were counted as described above by use of a fluorescence microscope (Nikon E800).

RESULTS

N-Ras is enriched in HCV replication complex-containing lipid rafts. We generated two stable Huh7 cell lines (SFL-2 and SFL-3) expressing a selectable full-length genome of HCV-1b. By flotation assay, we isolated nine fractions from both HCV replicon cell lines SFL-2 and SFL-3, from the T1 Huh7 clone expressing the neomycin resistance gene, and from Huh7 cells. The HCV proteins NS5A and NS5B and also caveolin-2, a marker of lipid rafts, were predominantly detected in the detergent-insoluble fractions (fraction 2). BiP, a non-raft membrane-associated protein residing in the endoplasmic reticulum, was recovered in heavier fractions (Fig. 1).

To characterize the protein contents of these detergent-insoluble fractions and to identify protein changes occurring as a result of HCV replication, we used two-dimensional polyacrylamide gel electrophoresis (2-D PAGE) followed by Q-TOF mass spectrometry. In order to optimize the resolution of

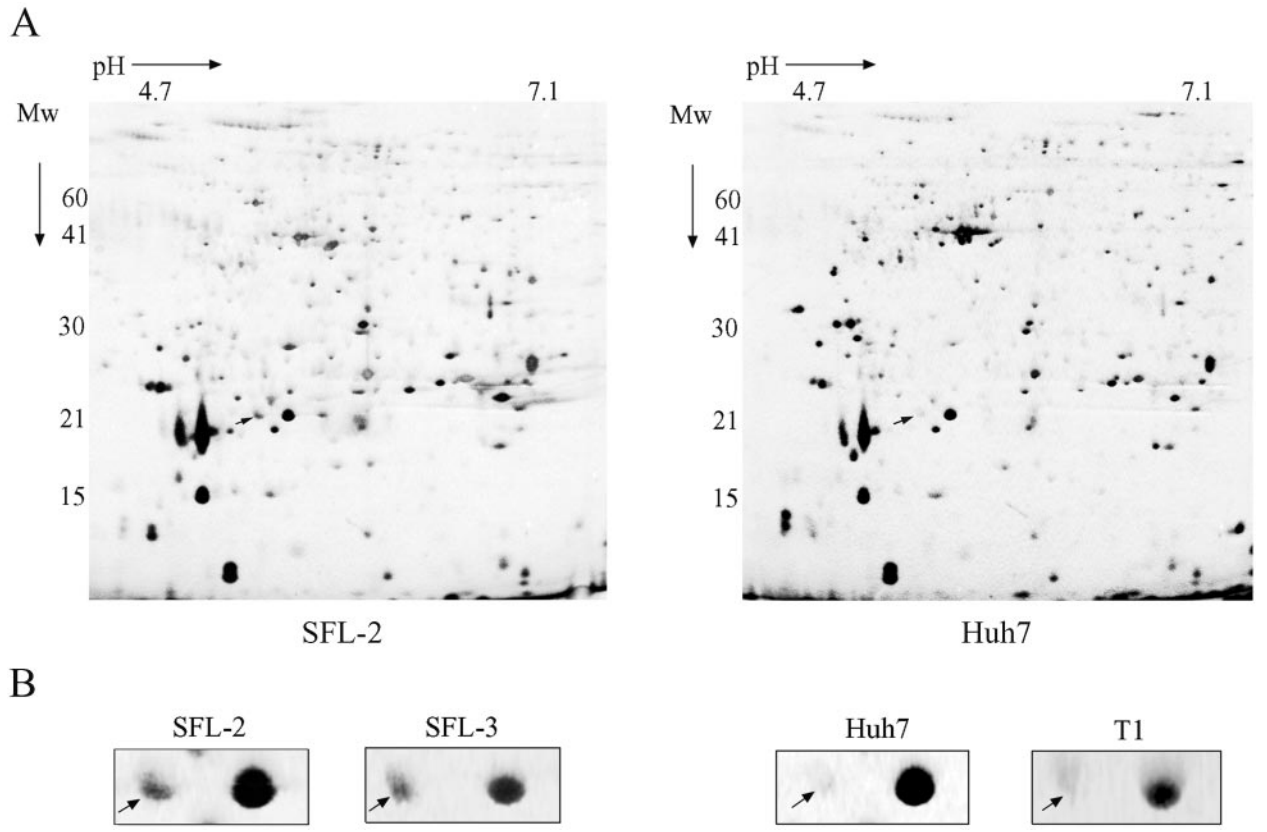

FIG. 2. (A) Representative silver-stained 2-D gels of detergent-resistant membrane fraction isolated from HCV replicon cell lines (left panel) and control cell lines (right panel). Proteins of the fraction were precipitated and solubilized in thiourea buffer containing 1% ASB-14 and separated by 2-D PAGE. An enhanced protein spot is marked with an arrow. Mw, molecular weight. (B) Close-up sections comparing the intensities of the selected spots in HCV replicon cell lines SFL-2 and SFL-3 and in Huh7 and T1 cells.

proteins from the lipid-enriched samples by 2-D PAGE, proteins in the detergent-insoluble fractions were precipitated with acetone-trichloroacetic acid and solubilized in thiourea buffer containing 1% ASB-14. Two independent experiments were performed to compare the protein content of lipid rafts isolated from replicon cell lines SFL-2 and SFL-3 and the protein content of lipid rafts isolated from control cell lines Huh7 and T1. Figure 2A shows typical 2-D patterns of proteins isolated from detergent-resistant fractions prepared from HCV replicon and control cell lines. Levels of 39 protein spots were modified in fraction 2 isolated from replicon cells compared to control cells, with 30 increased or new protein spots and 9 decreased spots (data not shown). In particular, the intensity of one protein spot with an apparent molecular mass of 21 kDa and pI of 5.3 was increased (mean ± standard deviation) by 5.75-fold ± 1-fold in the two replicon cell lines SFL-2 and SFL-3 in comparison to the spots from the two control cell lines, Huh7 and T1, in both experiments (Fig. 2B).

By Q-TOF mass spectrometry analysis, this protein spot was identified as N-Ras (Fig. 3A). The calculated molecular mass and pI of N-Ras are 21 kDa and 5.0, respectively, in agreement with the apparent molecular mass and pI of the increased spot. The increase of N-Ras in lipid rafts from HCV replicon cells was further confirmed by Western blot analysis (Fig. 3B). N-Ras levels in total protein lysates of HCV replicon clones and control cells were comparable (Fig. 3C), suggesting a redistribution of N-Ras into lipid rafts in HCV-replicating cells.

Activation of PI3K-Akt pathway in full-length HCV replicon cell lines. Cellular proto-oncogene N-Ras is a well-known activator of several signaling pathways. One of the N-Ras-dependent signaling pathways is the cell survival PI3K-Akt pathway (33). We investigated the possibility that the PI3K-Akt pathway may be activated in full-length HCV replicon cells. Activated PI3K generates PI(3,4,5)P3 phospholipids, which are necessary for the recruitment of Akt and PDK1 into membranes, and Akt is consequently phosphorylated by PDK1. Thus, activation of PI3K can be assessed by detection of the phosphorylated form of Akt (P-Akt). HCV-replicating SFL-2 and SFL-3 cells and control Huh7 and T1 cells were incubated in the presence or absence of serum, and levels of P-Akt were detected by Western blotting (Fig. 4A). When serum was present, P-Akt levels were enhanced (mean ± standard deviation) by 3.75-fold ± 0.35-fold in both HCV replicon cell clones in comparison to the levels of both controls in two experiments. Following serum deprivation, P-Akt in control cells was barely detectable, but significantly greater amounts of P-Akt were detected in HCV replicon cells. The overall levels of Akt in all cell lines were comparable.

To exclude potential clonal effects, transient transfection assays with HCV RNA in Huh7 cells were performed. P-Akt

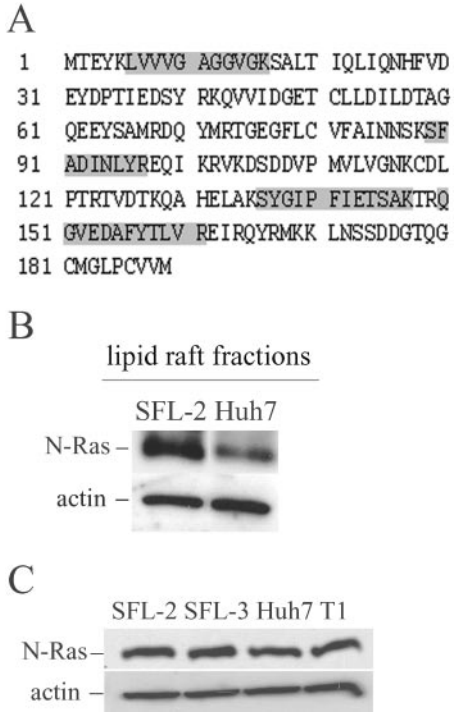

FIG. 3. Identification of N-Ras. (A) Peptides identified by Q-TOF mass spectrometry and their corresponding positions within the N-Ras sequence. (B) N-Ras protein levels in the detergent-resistant membrane fraction from the HCV replicon cell line SFL-2 and in Huh7 cells. N-Ras and actin were detected by Western blotting. (C) Western blot detection of N-Ras and actin in total cell lysates of replicon cell lines SFL-2 and SFL-3 and control cell lines Huh7 and T1.

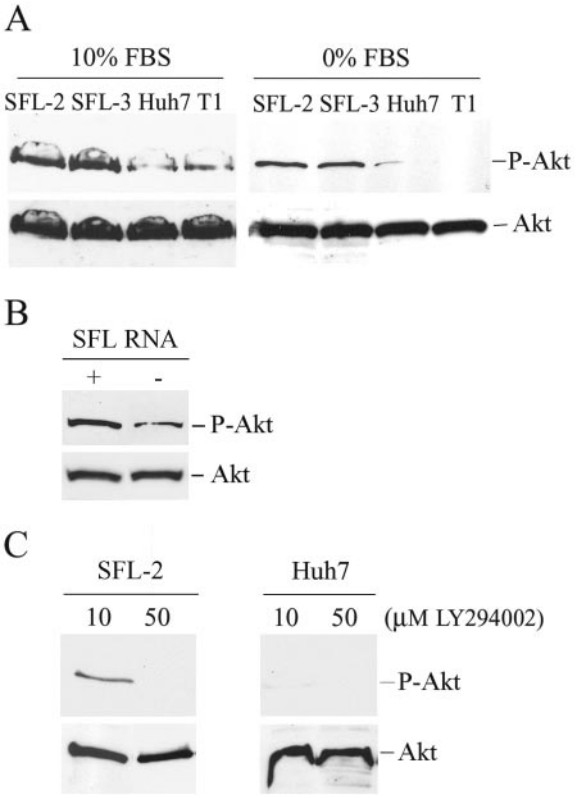

FIG. 4. Activation of PI3K and Akt in HCV replicon cell lines. (A) HCV replicon cell lines SFL-2 and SFL-3 and control cell lines Huh7 and T1 were incubated in the presence or absence of serum for 48 h. P-Akt and Akt were detected in cell lysates by Western blotting. (B) Huh7 cells were transiently transfected with an in vitro-transcribed sfl construct harboring full-length HCV genome (+) or mock transfected (−). P-Akt and Akt were detected in cell lysates by Western blotting. (C) The HCV replicon cell line SFL-2 and Huh7 cells were treated with 10 or 50 μM PI3K inhibitor LY294002 for 4 h. P-Akt and Akt were detected in cell lysates by immunodetection.

protein expression was determined 48 h posttransfection by Western blotting. We observed a 2.5-fold increase of P-Akt in Huh7-transfected cells in comparison to the amount in mock-transfected cells (Fig. 4B).

In addition, treatment of control Huh7 cells with 10 μM of the PI3K inhibitor LY294002 totally inhibited the phosphorylation of Akt, as expected. However, the same concentration of inhibitor only partially blocked the PI3K activity in HCV replicon cells, as indicated by the detection of P-Akt (Fig. 4C). A higher concentration of LY294002 (50 μM) resulted in a total inhibition of PI3K in both replicon and control cells. Akt levels were not affected by LY294002 treatment in replicon and control cells.

These results demonstrate that the activity of the PI3K-Akt pathway in HCV-replicating cells is induced.

Activation of mTOR in full-length HCV replicon cell lines. Mammalian target of rapamycin, mTOR, is regulated by the PI3K-Akt pathway (20). We previously reported that mTOR phosphorylates and consequently inactivates the translational repressor 4E-BP1 (4). To assess the activity of mTOR in HCV replicon cell lines, we wished to determine the extent of 4E-BP1 phosphorylation by Western blotting in three independent experiments. It has been previously reported that three isoforms of 4E-BP1 can be detected following immunoblotting, reflecting different phosphorylation states of this protein (4). In Huh7 control cells as well as in HCV-harboring Huh7 cells, only the phosphorylated isoforms of 4E-BP1 can be detected, suggesting a high level of activity of mTOR in these cells (Fig. 5A). In order to increase the sensitivity of detection of the phosphorylated 4E-BP1 isoforms by Western blotting, we used an antibody directed against phospho-4E-BP1. We detected increased amounts of phospho-4E-BP1 in HCV replicon SFL-2 and SFL-3 cells compared to that in control cells (increases in fold, 1.4 ± 0.1 and 1.5 ± 0.2, respectively) (Fig. 5A). Following serum deprivation, 4E-BP1 in Huh7 and T1 cells was entirely dephosphorylated as anticipated, whereas 4E-BP1 in HCV replicon cells was still phosphorylated (Fig. 5A). Following treatment with 10 μM of the PI3K inhibitor LY294002, phosphorylated 4E-BP1 isoforms were also detected in HCV replicon cells but not in control cells (data not shown).

To further confirm the increased activity of mTOR in HCV replicon cell lines, we assessed in two experiments the phosphorylation status of p70 S6 kinase (p70 S6K), another well-characterized substrate of mTOR (20). Phosphorylation of p70 S6K in replicon cells was increased (mean ± standard deviation) by 2.1-fold ± 0.4-fold and 2.7-fold ± 0.4-fold in comparison to Huh7 and T1 cells, respectively (Fig. 5B). Following serum deprivation, p70 S6K in Huh7 and T1 cells was dephosphorylated, whereas p70 S6K in HCV replicon cells remained

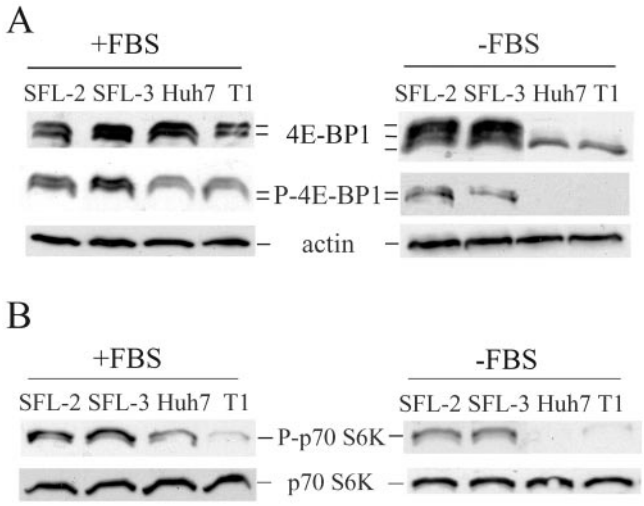

FIG. 5. Activation of mTOR in HCV replicon cell lines. Cells were incubated in the presence (+FBS) or absence (−FBS) of serum for 96 h. 4E-BP1, phosphorylated (P)-4E-BP1, p70 S6K, P-p70 S6K, and actin were detected by Western blotting. For 4E-BP1, the lower band and upper bands represent unphosphorylated and phosphorylated 4E-BP1 isoforms, respectively.

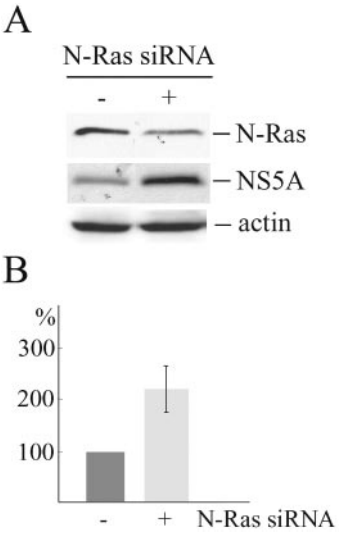

FIG. 7. Reduction of N-Ras protein expression by siRNA specific to N-Ras increases HCV replication. Replicon cells were transfected with siRNA (+) or with nontargeting siRNA (−). (A) After 30 h, cells were lysed and N-Ras, NS5A, and actin were visualized by Western blotting. (B) Total RNA was isolated and cDNA was synthesized by using HCV minus RNA strand-specific primer. Real-time PCR analysis of HCV RNA replication was performed using HCV 5′ nontranslated region-specific primers. The values represent the averages of three independent experiments ± standard deviations.

partially phosphorylated (Fig. 5B). Taken together, these results indicate that mTOR activity is stimulated in HCV-replicating cells.

Replicon cells are resistant to apoptosis. The role of PI3K-Akt in promoting cell survival has been largely documented (reviewed in references 10 and 15). More recently, regulation

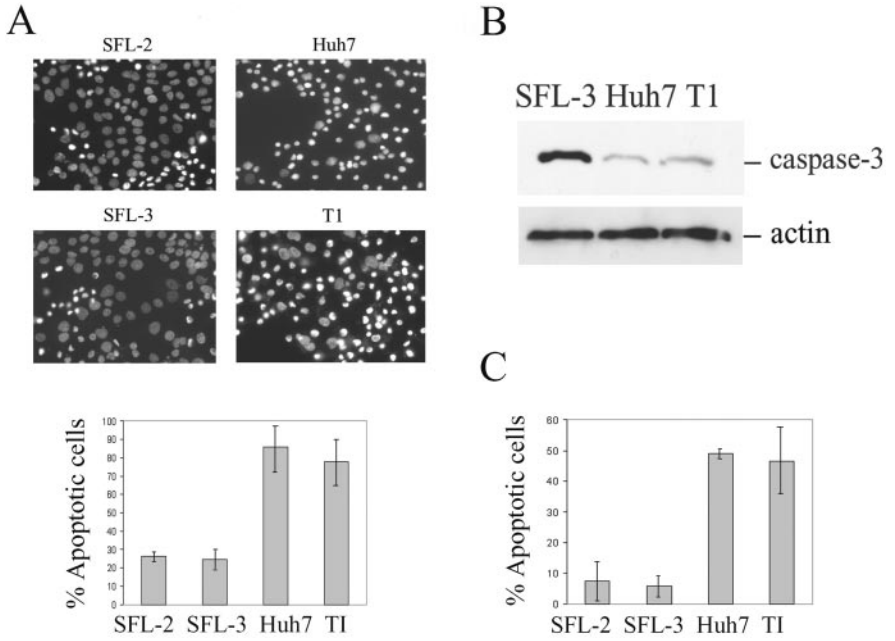

FIG. 6. HCV replicon cells are protected against apoptosis. (A) SFL-2, SFL-3, Huh7, and T1 cells were serum starved for 72 h before fixation and staining with Hoechst 33285 dye. Cells with bright, condensed, or fragmented nuclei were counted as apoptotic by use of fluorescence microscopy. The values represent means ± standard deviations from three independent experiments. (B) SFL-3, Huh7, and T1 cells were serum starved for 96 h, and caspase-3 was detected in cell lysates by Western blotting. A decrease of the amount of full-length caspase-3 indicates its cleavage and activation in Huh7 and T1 cells. (C) SFL-2, SFL-3, Huh7, and TI were serum starved for 72 h before fixation and TUNEL staining. The values represent the means ± standard deviations for positive cells from three independent experiments.

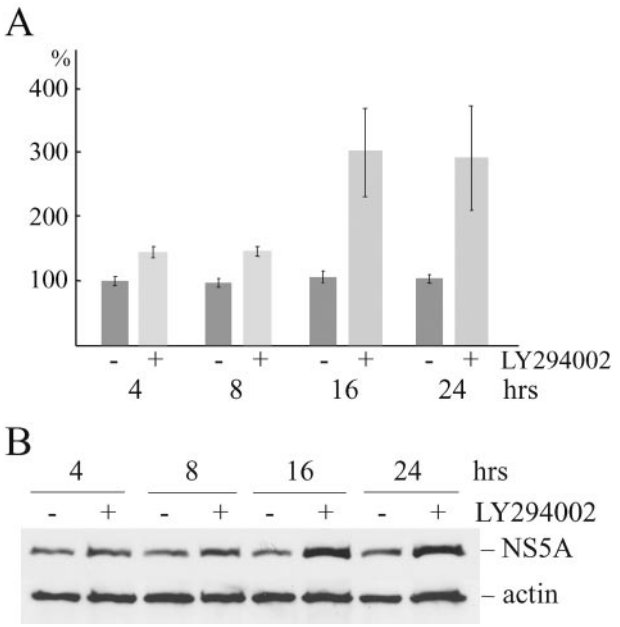

FIG. 8. Inhibition of PI3K activity increases HCV replication. Replicon cells were treated with 50 μM PI3K inhibitor LY294002 or vehicle for 4, 8, 16, and 24 h before lysis or total RNA isolation. (A) cDNA was synthesized by use of HCV minus RNA strand-specific primer and used for real-time PCR analysis with HCV 5′ non-translated region-specific primers. Average values from three experiments ± standard deviations are shown. (B) NS5A and actin were detected by Western blotting.

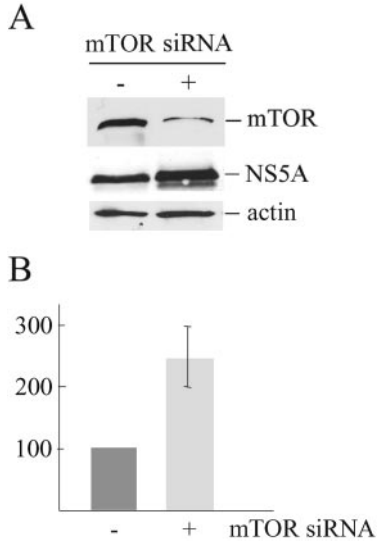

FIG. 9. Reduction of mTOR protein expression by siRNA specific to mTOR increases HCV replication. Replicon cells were transfected with mTOR siRNA (+) or nontargeting siRNA (−). (A) After 30 h, cells were lysed and mTOR, NS5A, and actin were detected by Western blotting. (B) Total RNA was isolated and cDNA was synthesized by use of HCV minus RNA strand-specific primer. Real-time PCR analysis was performed with HCV 5′ non-translated region-specific primers. Average values from three independent experiments ± standard deviations are shown.

of apoptosis by mTOR has also been suggested (40). To determine whether HCV replicon cells were protected against apoptosis as a consequence of PI3K-Akt-mTOR activation, SFL-2 and SFL-3 HCV replicon clones and Huh7 and T1 control cells were serum starved for 72 h and cell apoptosis was evaluated by three independent methods. The majority of Huh7 and T1 cells (86% ± 15.5% and 77.8% ± 11%, respectively) were scored as apoptotic by Hoechst dye staining in three independent experiments. In contrast, only 26.5% ± 2.2% and 24.5% ± 4.9% of SFL-2 and SFL-3 cells, respectively, were apoptotic (Fig. 6A). The observed differences between the two groups are statistically significant ($P = 0.004$).

Activation of caspase-3 was also assessed. Using Western blotting, we detected decreased amounts of full-length caspase-3 in Huh7 (by sixfold) and T1 (by fourfold) cells compared to the amounts in HCV replicon cells after prolonged serum starvation (Fig. 6B). The decrease of caspase-3 is indicative of its cleavage and consequent activation.

Finally, apoptosis was measured by TUNEL assay in three independent experiments. After the 72-h serum starvation, we detected 49% ± 1.4% and 46.5% ± 12% of TUNEL-positive Huh7 and T1 cells, respectively. In contrast, 7.3% ± 7% and 5.7% ± 3.1% of SFL-2 and SFL-3, respectively, were TUNEL positive ($P = 0.002$) (Fig. 6C). In conclusion, HCV replicon cells were largely resistant to induction of apoptosis by serum deprivation.

Effects of N-Ras, PI3K, and mTOR on HCV replication. We used specific siRNAs and inhibitors to assess the role of the N-Ras–PI3K–mTOR signaling pathway in HCV replication. Replicon cell lines were first transfected with siRNA specific to N-Ras or with nontargeting siRNA. Thirty hours posttransfection, N-Ras protein expression was reduced by approximately 60% in all three experiments performed (Fig. 7A). In replicon cells transfected with N-Ras siRNA, the amounts of HCV RNA were increased (mean ± standard deviation) by 2.1-fold ± 0.4-fold in comparison to the amounts in replicon cells transfected with nontargeting siRNA or mock transfected cells, as assessed by real-time PCR analysis of HCV RNA with the use of minus-strand-specific primer for cDNA synthesis (Fig. 7B). The amounts of NS5A detected in HCV replicon cells transfected with N-Ras siRNA were also greater (3-fold ± 0.07-fold) than the amounts in cells transfected with nontargeting siRNA or mock-transfected cells (Fig. 7A). Therefore, as determined at both the protein level and the genome level, replication of HCV in replicon cell lines was enhanced following the reduction of N-Ras protein levels.

To assess the effect of PI3K on HCV replication, replicon cells were treated with 50 μM of the PI3K inhibitor LY294002 for 4, 8, 16, and 24 h and replication of HCV was measured as described above. Inhibition of PI3K activity resulted in increased HCV RNA levels with significant effects after 16 and 24 h of treatment (means ± standard deviations were 3-fold ± 1-fold and 2.9-fold ± 1.1-fold, respectively) (Fig. 8A). NS5A protein levels were also significantly increased at 16 and 24 h of treatment (3.5-fold and 2.5-fold, respectively) (Fig. 8B).

Finally, we investigated the effect of mTOR on HCV replication. Replicon cells were transfected with siRNA mTOR, leading to a 75% reduction of mTOR protein levels 30 h posttransfection in all three experiments performed (Fig. 9A). HCV RNA and NS5A amounts were increased (mean ± stan-

dard deviation) by 2.4-fold ± 0.4-fold (Fig. 9B) and 2.5-fold (Fig. 9A), respectively, in replicon cells transfected with mTOR siRNA in comparison to nontargeting siRNA or mock-transfected cells.

Taken together, these data suggest that N-Ras signaling through the PI3K-Akt pathway and mTOR contribute to the maintenance of steady-state levels of HCV replication.

DISCUSSION

HCV replication complexes are associated with detergent-resistant membranes or lipid raft domains. Proteins associated with these rafts are key mediators of many biological events, such as trafficking and signaling. Proteins can be included in or excluded from rafts selectively, and the raft affinity of a given protein can be modulated by intracellular or extracellular stimuli. Lipid rafts also play important roles in the replication cycles of other viruses.

We therefore investigated the modification of the protein contents of lipid rafts in the presence of HCV. It is not possible to isolate lipid rafts in their native state; however, detergent-resistant membranes, containing clusters of many rafts, can be isolated by extraction with Triton X-100 or other detergents on ice and separated by centrifugation.

Using two-dimensional gel electrophoresis and mass spectrometry, we determined that N-Ras is enriched in HCV replication complex-containing, detergent-insoluble fractions. We also determined that the activities of the N-Ras downstream effectors PI3K, Akt, and mTOR in full-length HCV-1b genome-expressing stable cell lines were increased.

The regulatory subunit of PI3K, p85, is recruited into lipid rafts, and intact lipid rafts are important for the activation of PI3K-dependent signaling (27, 41). Activation of the PI3K-Akt pathway promotes cell survival in many cell types and mediates the survival function of N-Ras (reviewed in references 10 and 15). Modulation of this pathway is one of the strategies by which viruses inhibit apoptosis and prevent elimination of infected cells.

Viral proteins inducing PI3K-Akt-mediated inhibition of apoptosis include LMP1 of Epstein-Barr virus (13), human immunodeficiency virus type 1 Tat (14), middle T antigen of polyomavirus (12), and HBx of hepatitis B virus (23). Activation of the PI3K-Akt pathway as a consequence of constitutive activation of Ras by LMP2A of Epstein-Barr virus was also recently reported (30). For HCV, direct interaction between the nonstructural protein NS5A and the p85 subunit of PI3K, leading to its activation, has been described (21, 37). Our data suggest that activation of PI3K in stable cell lines expressing the full-length HCV genome may result from the enrichment of N-Ras in lipid rafts. In addition, activation of the N-Ras–PI3K–Akt pathway provided protection against apoptosis, in agreement with previous reports (37).

We also observed an increased level of activity of mTOR, a downstream target of PI3K-Akt, in HCV replicon cell lines. mTOR modulates translation by phosphorylation of the ribosomal p70 S6 kinase and of the translation initiation repressor 4E-BP1 (4, 20). Modulation of translation by mTOR differentially affects mRNAs, as demonstrated by differential recruitment of mRNAs to polysomes (19). Differential recruitment of mRNAs to polysomes was also observed following disruption of the Ras-Akt pathway (32). There is growing evidence that mTOR-dependent translational control may play a critical role in cell survival and transformation (2, 31, 40).

HCV establishes chronic infection in 80% of infected individuals. One of the hallmarks of chronic infection is stable, low-level virus replication. In stable HCV replicon cell lines cultured for prolonged periods, the level of HCV replication is constant (29; personal observation). This suggests that HCV develops a mechanism to maintain low steady-state levels of replication. Modulation of cell signaling might contribute to this process. Using specific siRNAs and inhibitors, we showed that HCV replication is increased by blockage of the N-Ras–PI3K–Akt–mTOR pathway at any level. This effect could be due to the modified translation efficiency of selective mRNAs. This effect could also be due to modification of the phosphorylation state of HCV viral proteins involved in virus replication. NS5A phosphorylation and HCV RNA replication have been recently described as being inversely correlated (16, 26). Although the kinases responsible for NS5A phosphorylation in vivo remain to be identified, Akt and the mTOR target, p70 S6 kinase, phosphorylate NS5A in vitro, and the inhibition of mTOR activity by rapamycin reduces NS5A phosphorylation (9). Therefore, activation of the PI3K-Akt-mTOR pathway may induce NS5A phosphorylation, leading to reduced HCV replication.

In conclusion, activation of the N-Ras–PI3K–Akt–mTOR signaling pathway may contribute not only to cell survival of HCV-infected cells but also to low steady-state levels of HCV replication, both of which may contribute to the establishment of persistent infection.

ACKNOWLEDGMENTS

We thank Ralf Bartenschlager for providing the sfl construct, Darius Moradpour for the anti-NS5B antibody, and Bin Deng and Samir Hanash for mass spectrometry analysis.

REFERENCES

1. **Aizaki, H., K.-J. Lee, V. M.-H. Sung, H. Ishiko, and M. M. C. Lai.** 2004. Characterization of the hepatitis C virus RNA replication complex associated with lipid rafts. Virology **324:**450–461.
2. **Avdulov, S., S. Li, V. Michalek, D. Burrichter, M. Peterson, D. M. Perlman, J. C. Manivel, N. Sonenberg, D. Yee, P. B. Bitterman, and A. A. Polunovsky.** 2004. Activation of translation complex eIF4F is essential for the genesis and maintenance of the malignant phenotype in human mammary epithelial cells. Cancer Cell **5:**553–563.
3. **Avota, E., N. Müller, M. Klett, and S. Schneider-Schaulies.** 2004. Measles virus interacts with and alters signal transduction in T-cell lipid rafts. J. Virol. **78:**9552–9559.
4. **Beretta, L., A. C. Gingras, Y. V. Svitkin, M. N. Hall, and N. Sonenberg.** 1996. Rapamycin blocks the phosphorylation of 4E-BP1 and inhibits cap-dependent initiation of translation. EMBO J. **15:**658–664.
5. **Blight, K. J., A. A. Kolykhalov, and C. M. Rice.** 2000. Efficient initiation of HCV RNA replication in cell culture. Science **290:**1972–1974.
6. **Briggs, J. A. G., T. Wilk, and S. D. Fuller.** 2003. Do lipid rafts mediate virus assembly and pseudotyping? J. Gen. Virol. **84:**757–768.
7. **Brown, G., C. E. Jeffree, T. McDonald, H. W. Rixon, J. D. Aitken, and R. J. Sugrue.** 2004. Analysis of the interaction between respiratory syncytial virus and lipid-rafts in Hep2 cells during infection. Virology **327:**175–185.
8. **Campbell, S., K. Gaus, R. Bittman, W. Jessup, S. Crowe, and J. Mak.** 2004. The raft-promoting property of virion-associated cholesterol, but not the presence of virion-associated Brij 98 rafts, is a determinant of human immunodeficiency virus type 1 infectivity. J. Virol. **78:**10556–10565.
9. **Coito, C., D. L. Diamond, P. Neddermann, M. J. Korth, and M. G. Katze.** 2004. High-throughput screening of the yeast kinome: identification of human serine/threonine protein kinases that phosphorylate the hepatitis C virus NS5A protein. J. Virol. **78:**3502–3513.
10. **Cox, A. D., and C. J. Der.** 2003. The dark side of Ras: regulation of apoptosis. Oncogene **22:**8999–9006.
11. **Cuadras, M. A., and H. B. Greenberg.** 2003. Rotavirus infectious particles

use lipid rafts during replication for transport to the cell surface in vitro and in vivo. Virology **313:**308–321.
12. **Dahl, J., A. Jurczak, L. A. Cheng, D. C. Baker, and T. L. Benjamin.** 1998. Evidence of a role for phosphatidylinositol 3-kinase activation in the blocking of apoptosis by polyomavirus middle T antigen. J. Virol. **72:**3221–3226.
13. **Dawson, C. W., G. Tramountanis, A. G. Eliopoulos, and L. S. Young.** 2003. Epstein-Barr virus latent membrane protein 1 (LMP1) activates the phosphatidylinositol 3-kinase/Akt pathway to promote cell survival and induce actin filament remodelling. J. Biol. Chem. **278:**3694–3704.
14. **Deregibus, M. C., V. Cantaluppi, S. Doublier, M. F. Brizzi, I. Deambrosis, A. Albini, G. Camussi.** 2002. HIV-1-Tat protein activates phosphatidylinositol 3-kinase/Akt-dependent survival pathways in Kaposi's sarcoma cells. J. Biol. Chem. **277:**25195–25202.
15. **Downward, J.** 2004. PI 3-kinase, Akt and cell survival. Semin. Cell Dev. Biol. **15:**177–182.
16. **Evans, M. J., C. M. Rice, and S. P. Goff.** 2004. Phosphorylation of hepatitis C virus nonstructural protein NS5A modulates its protein interactions and viral RNA replication. Proc. Natl. Acad. Sci. USA **101:**13038–13043.
17. **Girard, S., P. Shalhoub, P. Lescure, A. Sabile, D. E. Misek, S. Hanash, C. Brechot, and L. Beretta.** 2002. An altered cellular response to interferon and up-regulation of interleukin-8 induced by the hepatitis C viral protein NS5A uncovered by microarray analysis. Virology **295:**272–283.
18. **Gosert, R., D. Egger, V. Lohmann, R. Bartenschlager, H. E. Blum, K. Bienz, and D. Moradpour.** 2003. Identification of the hepatitis C virus RNA replication complex in Huh-7 cells harboring subgenomic replicons. J. Virol. **77:**5487–5492.
19. **Grolleau, A., J. Bowman, B. Pradet-Balade, E. Puravs, S. Hanash, J. A. Garcia-Sanz, and L. Beretta.** 2002. Global and specific translational control by rapamycin in T-cells uncovered by microarrays and proteomics. J. Biol. Chem. **277:**22175–22184.
20. **Hay, N., and N. Sonenberg.** 2004. Upstream and downstream of mTOR. Genes Dev. **18:**1926–1945.
21. **He, Y., H. Nakao, S.-L. Tan, S. J. Polyak, P. Neddermann, S. Vijaysri, B. L. Jacobs, and M. G. Katze.** 2002. Subversion of cell signaling pathways by hepatitis C virus NS5A via interaction with Grb2 and p85 PI3K. J. Virol. **76:**9207–9217.
22. **Helms, J. B., and C. Zurzolo.** 2004. Lipids as targeting signals: lipid rafts and intracellular trafficking. Traffic **5:**247–254.
23. **Lee, Y. I., S. Kang-Park, and S. I. Do.** 2001. The hepatitis B virus-X protein activates a phosphatidylinositol 3-kinase-dependent survival signaling cascade. J. Biol. Chem. **276:**16969–16977.
24. **Lohmann, V., F. Körner, J. O. Koch, U. Herian, L. Theilmann, and R. Bartenschlager.** 1999. Replication of subgenomic hepatitis C virus RNAs in a hepatoma cell line. Science **285:**110–113.
25. **Mañes, S., G. del Real, and C. Martínez-A.** 2003. Pathogens: raft hijackers. Nat. Rev. Immunol. **3:**557–568.
26. **Neddermann, P., M. Quintavalle, C. Di Pietro, A. Clementi, M. Cerretani, S. Altamura, and R. De Francesco.** 2004. Reduction of hepatitis C virus NS5A hyperphosphorylation by selective inhibition of cellular kinases activates viral RNA replication in cell culture. J. Virol. **78:**13306–13314.
27. **Peres, C., A. Yart, B. Perret, J.-P. Salles, and P. Raynal.** 2003. Modulation of PI3K activation by cholesterol level suggests a novel positive role for lipid rafts in lysophosphatidic acid signaling. FEBS Lett. **534:**164–168.
28. **Pietschmann, T., V. Lohmann, A. Kaul, N. Krieger, G. Rinck, G. Rutter, D. Strand, and R. Bartenschlager.** 2002. Persistent and transient replication of full-length hepatitis C virus genomes in cell culture. J. Virol. **76:**4008–4021.
29. **Pietschmann, T., V. Lohmann, G. Rutter, K. Kurpanek, and R. Bartenschlager.** 2001. Characterization of cell lines carrying self-replicating hepatitis C virus RNAs. J. Virol. **75:**1252–1264.
30. **Portis, T., and R. Longnecker.** 2004. Epstein-Barr virus LMP2A mediates B-lymphocyte survival through constitutive activation of the Ras/PI3K/Akt pathway. Oncogene **23:**8619–8628.
31. **Rajasekhar, V. K., and E. C. Holland.** 2004. Postgenomic global analysis of translational control induced by oncogenic signaling. Oncogene **23:**3248–3264.
32. **Rajasekhar, V. K., A. Viale, N. D. Socci, M. Wiedmann, X. Hu, and E. C. Holland.** 2003. Oncogenic Ras and Akt signaling contribute to glioblastoma formation by differential recruitment of existing mRNAs to polysomes. Mol. Cell **12:**889–901.
33. **Rodriguez-Viciana, P., P. H. Warne, R. Dhand, B. Vanhaesebroeck, M. D. Waterfield, and J. Downward.** 1994. Phosphatidylinositol-3-OH kinase is a direct target of Ras. Nature **370:**527–532.
34. **Schmitt, A. P., and R. A. Lamb.** 2004. Escaping from the cell: assembly and budding of negative-strand RNA viruses. Curr. Top. Microbiol. Immunol. **283:**145–196.
35. **Shi, S. T., K.-J. Lee, H. Aizaki, S. B. Hwang, and M. M. C. Lai.** 2003. Hepatitis C virus RNA replication occurs on a detergent-resistant membrane that cofractionates with caveolin-2. J. Virol. **77:**4160–4168.
36. **Simons, K., and D. Toomre.** 2000. Lipid rafts and signal transduction. Nat. Rev. Mol. Cell Biol. **1:**31–39.
37. **Street, A., A. Macdonald, K. Crowder, and M. Harris.** 2004. The hepatitis C virus NS5A activates a PI3K-dependent survival signaling cascade. J. Biol. Chem. **279:**12232–12241.
38. **Suomalainen, M.** 2002. Lipid rafts and assembly of enveloped viruses. Traffic **3:**705–709.
39. **Triantafilou, K., and M. Triantafilou.** 2003. Lipid raft microdomains: key sites for Coxsackievirus A9 infection cycle. Virology **317:**128–135.
40. **Wendel, H. G., E. de Stanchina, J. S. Fridman, A. Malina, S. Ray, S. Kogan, C. Cordon-Cardo, J. Pelletier, and S. W. Lowe.** 2004. Survival signalling by Akt and eIF4E in oncogenesis and cancer therapy. Nature **428:**32–337.
41. **Zhuang, L., J. Lin, M. L. Lu, K. R. Solomon, and M. R. Freeman.** 2002. Cholesterol-rich lipid rafts mediate akt-regulated survival in prostate cancer cells. Cancer Res. **62:**2227–2231.